




Cite this: *Environ. Sci.: Water Res. Technol.*, 2021, 7, 638

## Removal of PFASs from biosolids using a semi-pilot scale pyrolysis reactor and the application of biosolids derived biochar for the removal of PFASs from contaminated water†

Sazal Kundu, <sup>a</sup> Savankumar Patel, <sup>a</sup> Pobitra Halder, <sup>a</sup> Tejas Patel, <sup>a</sup> Mojtaba Hedayati Marzbali, <sup>a</sup> Biplob Kumar Pramanik, <sup>b</sup> Jorge Paz-Ferreiro, <sup>a</sup> Cícero Célio de Figueiredo, <sup>c</sup> David Bergmann,<sup>d</sup> Aravind Surapaneni, <sup>de</sup> Mallavarapu Megharaj <sup>fg</sup> and Kalpit Shah <sup>\*ae</sup>

This study focuses on the conversion of biosolids to biochar and its further use in adsorbing per- and polyfluoroalkyl substances (PFASs) from contaminated water. In particular, this study aims to (a) investigate the performance of a semi-pilot fluidised bed pyrolysis unit in converting biosolids into biochar, (b) examine the ability of the pyrolysis–combustion integrated process to destruct PFASs present in biosolids and (c) study the application of biosolids derived biochar for removing PFASs from contaminated water. The semi-pilot fluidised bed pyrolysis unit demonstrated stable temperature and oxygen profiles in the reactor. The yield of biochar was found to be 36–45% at studied temperatures (500–600 °C). The produced biosolids derived biochar samples, due to their lower H/C and O/C ratio, were found to be extremely stable with an expected long (millennia) residence time in soil. It was concluded that >90% removal of perfluorooctanesulfonate (PFOS) and perfluorooctanoic acid (PFOA) from biosolids derived biochar could be achieved in the pyrolysis–combustion integrated process. The biosolids derived biochar demonstrated >80% adsorption of long-chain PFASs and 19–27% adsorption of short-chain PFASs from PFAS contaminated water.

Received 16th August 2020,  
Accepted 16th December 2020

DOI: 10.1039/d0ew00763c

rs.li/es-water

### Water impact

The effectiveness of a fluidised bed pyrolysis for reducing biosolids volume and producing biochar material was demonstrated. Over 90% of PFOS and PFOA was safely removed from the resultant biochar during pyrolysis. The produced biochar was able to adsorb PFASs from contaminated water in the range of 20 to over 95%, depending on the individual PFAS considered.

## 1. Introduction

Stabilised sewage sludge, produced by wastewater treatment plants (WWTPs), is known as biosolids. This material is an unavoidable by-product that originates from households and many industries.<sup>1</sup> The rapid increase in population as well as urbanisation contributes to a continued increase in the production of biosolids.<sup>2,3</sup> Biosolids contain many macronutrients such as nitrogen, phosphorus, sulphur, potassium, calcium and magnesium as well as micronutrients such as zinc, copper, boron, molybdenum, manganese and iron.<sup>4</sup> Therefore, biosolids are attractive for agricultural applications, and the majority of this material is currently utilised for this purpose in many countries including Australia.<sup>5,6</sup> However, biosolids may contain harmful pathogens and current regulations (particularly in

<sup>a</sup> Chemical & Environmental Engineering, School of Engineering, RMIT University, Melbourne, Victoria 3000, Australia. E-mail: kalpit.shah@rmit.edu.au;

Fax: +61 3 9925 7110; Tel: +613 9925 1109

<sup>b</sup> Civil and Infrastructure Engineering, School of Engineering, RMIT University, Melbourne, Victoria 3000, Australia

<sup>c</sup> Faculty of Agronomy and Veterinary Medicine, University of Brasília, 70910-970 Brasília, DF, Brazil

<sup>d</sup> South East Water, Frankston, Victoria 3199, Australia

<sup>e</sup> ARC Training Centre for Transformation of Australia's Biosolids Resource, RMIT University, Bundoora, Victoria 3083, Australia

<sup>f</sup> Global Centre for Environmental Remediation, Faculty of Science, University of Newcastle, Callaghan, NSW 2308, Australia

<sup>g</sup> Cooperative Research Centre for Contamination Assessment and Remediation of the Environment (CRC CARE), Callaghan, NSW 2308, Australia

† Electronic supplementary information (ESI) available. See DOI: 10.1039/d0ew00763c

Victoria, Australia) require biosolids to be stockpiled onsite for 1–3 years to reduce pathogen levels to the highest possible treatment grade for soil amendment. Also, heavy metals, micro-plastics, pesticides, chemicals, herbicides and pharmaceutical ingredients are present in biosolids.<sup>2,3,7</sup> Recently, biosolids have been recognised as a potential source of PFAS contamination in soil and groundwater which may restrict their land application in the near future.<sup>8,9</sup>

PFASs are anthropogenic compounds and, historically, have been used in a wide range of applications including fire-fighting foams, non-stick cookware, stain- and water-repellent fabrics, polishes, waxes, paints and cleaning products.<sup>10,11</sup> To date, more than 3000 PFASs and their potential precursors have been identified<sup>12</sup> and their numbers increase with time as research progresses. Consequently, PFASs have become ubiquitous in terrestrial and aquatic environments. These chemicals are persistent, accumulative and leachable. PFOA and PFOS are the most-studied PFASs. Humans may introduce PFASs in their bodies *via* drinking contaminated water, and eating fish and meat as well as vegetables and fruits. The adverse effects of PFAS in human bodies may include, but are not limited to, increased cholesterol,<sup>13</sup> hepatotoxicity and alterations in the immune system<sup>14</sup> as well as thyroid hormone disruption.<sup>15</sup> Besides, these chemicals may cause low infant birth weights,<sup>16</sup> and they are also suspected of causing cancer.<sup>17</sup>

PFASs have been detected in WWTP influent, effluent and biosolids globally.<sup>18</sup> Hydrophobic partitioning in WWTPs is expected to result in the retention of long-chain PFASs in the sludge/biosolids.<sup>19</sup> The major PFASs in biosolids, reported in a study on US biosolids, were PFOS ( $403 \pm 127 \text{ ng g}^{-1}$  dry weight) and PFOA ( $34 \pm 22 \text{ ng g}^{-1}$  dry weight).<sup>19</sup> The other PFAS values were lower and in the range of 2 and  $26 \text{ ng g}^{-1}$  dry weight. Similar results were obtained in Australian studies.<sup>9,20</sup> PFAS management guidelines have become available in several Australian states, for example, in Victoria (regulated by EPA Victoria).<sup>8</sup> These may potentially impact the wider land application of biosolids in the near future. Therefore, a reliable and cost-effective technological platform is warranted that minimises/eliminates the PFAS risks of biosolids for land application.

PFASs have strong chemical structures, are thermally very stable and require high reaction energy/high temperatures to break down their chemical bonds. The available literature suggests that immobilisation could be the most cost-effective method for remediation of PFASs in biosolids and biosolids amended soils.<sup>21</sup> However, keeping PFASs immobilised in a solid matrix for a long time still needs to be verified by further investigation. Thermal treatments such as pyrolysis, gasification, combustion and incineration may have the potential to fully/partially destruct PFASs due to their high temperature operation conditions. Most of the studies in the literature have focused on investigating PFAS destruction through incineration.<sup>22–26</sup> Studies on the potential of pyrolysis and gasification technologies to destruct PFASs are very limited.

The pyrolysis process decomposes carbonaceous materials, such as biosolids, in the absence of oxygen.<sup>2</sup> Usually, a sweeping gas flow is provided in the pyrolysis process (except vacuum pyrolysis). In the case of fluidised bed pyrolysis, the flow-rate of the sweeping gas is high and it may be economically feasible to recycle the CO<sub>2</sub> containing hot pyrolysis/flue gas as the sweeping gas rather than using a high purity and expensive inert sweeping gas such as N<sub>2</sub>. Biochar (solid), bio-oil (liquid) and bio-gas are the three products that are generated from the pyrolysis of biosolids. The yield distribution of these products depends on a number of parameters including the composition of biosolids, pyrolysis temperature, heating/energy transfer rate, and flow rate of the sweeping gas as well as the catalyst/additive if used. Bio-oil and bio-gas could be used as fuel<sup>24,27</sup> while biochar could be used as a soil amendment material,<sup>24,27</sup> as a catalyst in the production of carbon nanomaterials<sup>28</sup> or as an adsorbent for removing micropollutants.<sup>29,30</sup> If there is a priority between biochar and bio-oil, the heating/energy transfer rate is usually considered to be tweaked. When bio-oil is considered to be the primary product, a high heating rate is applied while a slow heating rate is applied when biochar is considered to be the primary product. Previous studies suggested that pyrolysis can successfully destroy impurities such as pathogens, micro-plastics, pesticides and pharmaceutical ingredients and the products from this process can be free from these nuisances.<sup>31–34</sup> If the destruction of PFASs from biosolids can be safely performed by a pyrolysis process, it can assist water industries in reducing biosolids volume and creating an indisputable application of biosolids derived biochar as a soil amendment material as well as its other applications in chemical processing.

Pyrolysis can be carried out in both fixed bed and fluidised bed reactors. The poor gas–solid contact in fixed bed reactors may compromise the quality of biochar. Biochar with uniform characteristics is beneficial and desired, particularly if the considered end use is being a catalyst or an adsorbent. Fluidised bed reactors ensure uniform heating even at high heating rates leading to the production of high quality biochar with uniform characteristics. This opens up the possibility of extending the application of biosolids derived biochar, produced from fluidised bed reactors, in the adsorption of PFASs from contaminated water.

Several reactor designs have been evaluated in a large scale for the pyrolysis of biosolids. For instance, a microwave heating system was applied aiming to produce bio-oil as a primary product from the transformation of sewage sludge using several additives such as KOH, H<sub>2</sub>SO<sub>4</sub>, H<sub>3</sub>BO<sub>3</sub>, ZnCl<sub>2</sub> and FeSO<sub>4</sub>.<sup>35</sup> The technological feasibility was found to be dependent on the optimisation of process parameters and selection of appropriate additives. In a different study, sewage sludge was blended with other feedstock such as manure and studied in a fixed bed pilot-scale reactor with positive findings.<sup>36</sup> A few other pilot-scale studies were carried out using a fixed bed reactor in non-catalytic, autocatalytic or catalytic mode. However, the application of

fluidised bed pyrolysis reactors is found to be rare for pyrolysis of biosolids. In addition, pyrolysis is an endothermic process and the optimisation of energy is vital for the commercial viability of any technology. Therefore, a fluidised bed pilot scale reactor integrated with a combustion chamber, which aims to run pyrolysis in autothermal mode (*i.e.* no need for external energy), is in demand in the search for sustainable uses of biosolids.

Typically, pyrolysis of carbonaceous materials is carried out between 300 to 1000 °C.<sup>37</sup> Lower pyrolysis temperature generates biochar with a lower surface area and high oxygen containing functional groups. As the pyrolysis temperature increases, the surface area of biochar increases at the expense of functional groups. Therefore, low temperature pyrolysis is generally preferred for producing biochar for soil application while high temperature is desired when biochar with a high surface area needs to be produced. Choosing a pyrolysis temperature is challenging and a few aspects could be taken into consideration. (a) This work aims to produce biochar to be used as an adsorbent; therefore, a high surface area and an improved morphology is critical. Our previous work suggests that the pyrolysis temperature has a tremendous impact on the morphology of biochar and a pyrolysis temperature between 500 and 700 °C can generate biochar with a high porosity and surface area from biosolids.<sup>28</sup> (b) The second aspect may be the destruction of pollutants, particularly PFASs which are inherently present in biosolids. The devolatilisation and destruction of PFASs at high temperature during combustion have been established.<sup>38,39</sup> However, biosolids contain a reasonable concentration of metals and minerals that are expected to function as catalysts for the destruction of PFASs at relatively low temperature in an integrated pyrolysis–combustion process which has not been studied in the literature. (c) The third aspect may be the formation of polycyclic hydrocarbons (PAHs). Below 500 °C pyrolysis temperature, PAHs are formed *via* carbonisation and aromatisation.<sup>40,41</sup> Above 500 °C, a free radical pathway, followed by pyrosynthesis, dominates the formation of PAHs.<sup>40–42</sup> When investigating PAH formation in the pyrolysis temperature range of 100–700 °C, researchers found that the formation of PAHs is the highest in the temperature range of 400–500 °C.<sup>43,44</sup> Applying a pyrolysis temperature  $\geq 500$  °C is often suggested to minimise extractable PAHs in biochar.<sup>43,45</sup> Accounting for all these aspects, a moderate temperature range of 500–600 °C could be considered which is a trade-off between minimising PAHs and obtaining high quality biochar while assisting in the investigation of destruction of PFASs in biosolids at relatively low temperature.

PFAS contamination in ground water and industrial wastewater is a serious problem and their concentrations often reach above those set by the regulatory guidelines.<sup>46</sup> So far, granular activated carbon (GAC) from various sources (*e.g.*, coconut shell and coal) has been extensively studied for the adsorption of PFASs.<sup>46–50</sup> Biomass derived biochar has also been used in PFAS adsorption studies.<sup>51,52</sup> However, biosolids derived biochar has been rarely used in adsorption studies of PFASs.

The aim of the current study is to (a) investigate the performance of a semi-pilot fluidised bed pyrolysis unit in converting biosolids into biochar, (b) examine the ability of the pyrolysis–combustion integrated process to destruct PFASs present in biosolids and (c) study the application of biosolids derived biochar for removing PFASs from contaminated water.

## 2. Methodology

### 2.1. Pyrolysis of biosolids

**2.1.1. Biosolids sample.** The biosolids sample employed in this study was sourced from the Mount Martha Water Recycling Plant (38°16'06"S and 145°03'31"E) of South East Water Corporation, Victoria, Australia. This plant predominantly receives domestic and trade sewage, and treats sewage sludge through an activated sludge process followed by anaerobic digestion. After digestion, the solids are processed through a dewatering plant (*i.e.*, centrifuge) and solar drying facility before they are sent to stockpiling. Thus, the samples used in this study were processed through a solar dryer shed.

The biosolids sample was initially ground using a pin mill (Chenwei Machinery CW-20B) and then segregated using a vibrating screen (Sanfeng Machinery, SF-600) at FA Maker Pty. Ltd., Victoria, Australia. The pin mill and vibrating screen employed in this study are shown in Fig. S1† The biosolids, used in the trials, were 0.5–2 mm in particle size. The detailed proximate and ultimate analyses of biosolids are presented in Table 1.

**2.1.2. Description of the semi-pilot unit employed for the pyrolysis of biosolids.** The process block diagram is shown in Fig. 1 (actual image of the semi-pilot pyrolysis plant can be found in ESI† Fig. S2). Each pyrolysis trial was conducted for 5 hours. Trials were performed in triplicate ( $n = 3$  for each trial) to ensure consistency of the data and the average values are presented in this manuscript. The run mode of this system is considered as semi-continuous since the biosolids

**Table 1** Proximate and ultimate analyses of biosolids

Proximate analysis <sup>a</sup> (%)				Ultimate analysis <sup>a</sup> (%)				
Moisture	Volatiles	Ash	Fixed carbon	C	H	N	S	O <sup>b</sup>
11.0	60.6	29.0	10.4	38.3	4.7	6.02	0.96	21.02

<sup>a</sup> Values on a dry weight basis. <sup>b</sup> Value determined by difference.

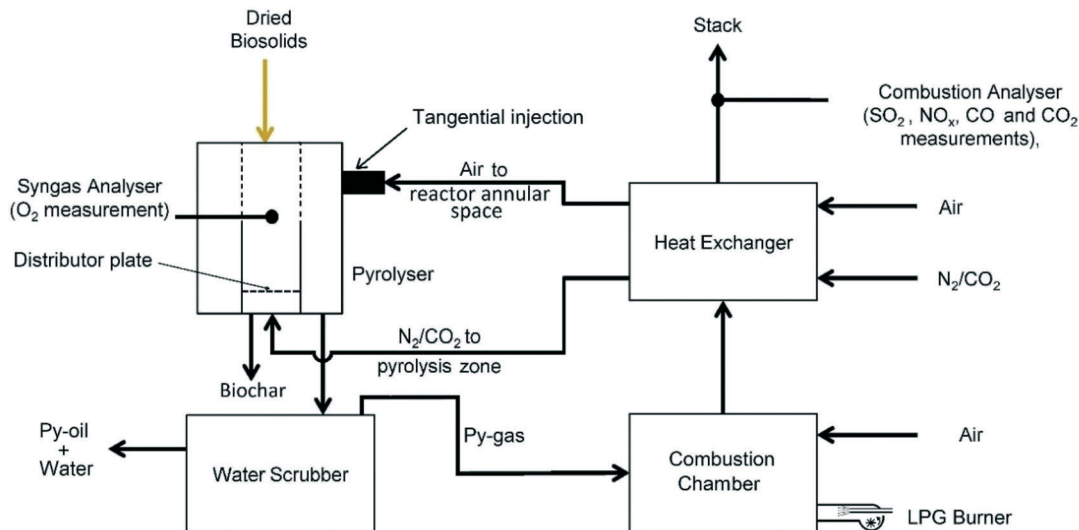


Fig. 1 Process block diagram for the semi-pilot plant setup.

were fed continuously throughout the trial period while char was collected only after the 5-hour period at the end of each trial.

During start-up, the semi-pilot plant was heated *via* a liquefied petroleum gas (LPG) burner. The hot flue gas leaving the LPG burner was used to pre-heat the gases (*i.e.* air and  $N_2/CO_2$ ) entering the semi-pilot plant *via* a heat exchanger. The pre-heated air and  $N_2/CO_2$  gases were then circulated in the reactor to heat the reactor to a desired temperature. The hopper was filled with the biosolids sample at the beginning of each trial (Fig. S2†). The hopper was charged with  $N_2$  *via* a  $N_2$  purging line. Once the desired temperature of the reactor was attained, biosolids were continuously charged at  $0.25 \text{ kg h}^{-1}$  from the hopper to the reactor *via* a pre-calibrated screw-feeder with continuous  $N_2$  purging. The screw-feeder was calibrated for each trial.

The reactor, employed in this study, was constructed from stainless steel 253MA and insulated with ceramic fibre insulation to minimise heat losses. It was of concentric geometry, where the inner tube functioned as the pyrolyser. The bottom half of the inner tube was made of pipe, while the top half of the inner tube consisted of a wedge-wire screen. Biosolids were pyrolysed under bubbling fluidised conditions using a pre-heated  $N_2/CO_2$  mixed stream containing 85%  $N_2$  and 15%  $CO_2$ , v/v. The reason for using a  $N_2/CO_2$  mixed stream (85%  $N_2$ , 15%  $CO_2$ , v/v) in the pyrolyser was to mimic the scenario of pyrolysis in the presence of recycled flue gas. The produced gas and oil vapours from the inner pyrolyser tube were then transferred to the annular space *via* the wedge-wire screen from the top half of the reactor while the biochar produced remained at the bottom of the inner pyrolyser tube. At the end of each trial, biochar was kept further in that inner tube with an inert environment for cooling and then collected further for analysis. The annular space acted as a partial combustor for py-gas and py-oil vapours. The temperature in the annular space was

controlled by adjusting the air inlet rate. The temperature at the annular space was purposefully kept lower or equal to the pyrolysis temperature to find out whether or not PFASs are destroyed at lower temperatures in thermal systems.

By employing pre-heated air tangentially at a  $>10 \text{ m s}^{-1}$  velocity in the annular space, the py-gas and py-oil vapours were partially combusted and PFASs, if they survived in the pyrolyser, were destructed in this annular space. The remaining py-gas and py-oil vapours were rapidly transported from the annular space to a water scrubber, where they were immediately quenched. The reason for using tangential entry and high-velocity air was to ensure that the pyrolysis reaction environment is not affected and the py-gas and py-oil vapours are immediately quenched without any secondary reactions. The py-oil was condensed in the scrubber water, while non-condensable py-gas was sent to the combustion chamber of the LPG burner to ensure that it was combusted before releasing to the environment. The energy required for pyrolysis was provided by the hot air and  $N_2/CO_2$  gases, which were pre-heated using the combustion of LPG and py-gas (once produced). At the end of each trial, the sample from the water scrubber was collected for oil and PFAS analysis. Any PFAS species carried by the gas stream, if they survive in the pyrolysis–combustion system, should be trapped in the water scrubber. The reason is that the boiling points of PFASs, even for short chain PFASs (*e.g.*, the boiling point of pentafluorobenzoic acid (PFBA) is  $220 \text{ }^\circ\text{C}$ ), are higher than the water boiling point.

An online gas monitor (combustion analyser, MRU Optima 7) was employed to measure the concentrations of various gaseous species ( $CO$ ,  $CO_2$ ,  $NO_x$  and  $SO_x$ ) in the stack. The reactor was equipped with four thermocouples and they measured the following temperatures: 1) pyrolyser temperature, 2) annular space temperature, 3) reactor inlet  $N_2/CO_2$  stream temperature and 4) reactor inlet  $N_2$  temperature. The pyrolysis trials were carried out at three different temperatures: 500, 550



and 600 °C. The average temperature at the pyrolyser thermocouple was considered as the pyrolysis temperature. The concentration of O<sub>2</sub> in the pyrolyser was continuously monitored by an online gas monitor (syngas analyser, Madur Aqua GA40T Plus). Biochar produced from biosolids in the semi-pilot trials at 500, 550 and 600 °C are labelled as BSBC-500, BSBC-550 and BSBC-600, respectively.

Biochar produced during the trial was characterised by surface imaging using a scanning electron microscope (SEM) of the Philips XL30 model and a Brunauer–Emmett–Teller (BET) analyser (Micromeritics 2000/2400). The particle size distributions of both biosolids and biochar were determined using a Malvern particle size analyser (Mastersizer 3000). Analyses related to PFAS, py-oil and heavy metals were performed externally (by ALS Limited, Australia). ALS laboratories are NATA (National Association of Testing Authorities, Australia) accredited laboratories. They have applied their WP045B, WP075A and WP0125A methods for py-oil analysis, EP231 method for PFAS analysis and WG020B for heavy metal analysis.

## 2.2. PFAS adsorption

**2.2.1. Biochar preparation for PFAS adsorption.** Biomass biochar was produced at 600 °C pyrolysis temperature to make a comparison with biosolids biochar produced at the same temperature (BSBC-600) mainly for exploring its potential to adsorb PFASs from PFAS contaminated water. The biomass biochar produced at 600 °C in this study is referred to as BMBC-600. Sawdust (predominantly Australian pine wood, sourced from a mechanical workshop at RMIT University) of the same initial particle size as the biosolids (*i.e.*, 0.5–2 mm) was used in the production of biomass biochar. Instead of a semi-pilot plant, a muffle furnace (Barnstead Thermolyne 30400) was employed for the production of biomass biochar, where the furnace was operated at 600 °C for 1 hour. The furnace was then kept closed until it was cooled down naturally to room temperature. Afterwards, the biochar sample was taken out and stored in a desiccator. Both BMBC-600 and BSBC-600 were sieved to obtain a particle size of 0.3–0.5 mm and further employed in the PFAS adsorption study. The BET surface areas of these samples were measured and found to

be 79.87 m<sup>2</sup> g<sup>-1</sup> and 55.29 m<sup>2</sup> g<sup>-1</sup> for BMBC-600 and BSBC-600, respectively.

**2.2.2. Procedure for PFAS adsorption.** Two PFAS contaminated water samples (sources can't be revealed) were used in this study. The PFAS content in sample 1 was significantly higher than that in sample 2 (Table 2). In addition, several PFAS species in sample 2 were below the detection limit of the analytical instrument, and therefore, they were excluded from the adsorption study. The pH values of sample 1 and sample 2 were 4.3 and 7.85, respectively. In this study, we have not adjusted the pH level for the adsorption tests.

Initially, PFAS contaminated water samples were filtered through 6-micron polyethersulfone (PES) membrane filter paper to remove any suspended solids. Two adsorbents were employed to remove PFASs from these samples as detailed earlier: 1) biosolids biochar (BSBC-600) and 2) biomass biochar (BMBC-600). For each study, one gram of adsorbent was taken in a conical flask, and 50 mL of PFAS contaminated water was introduced into the conical flask. For each set of adsorption study, there was a repeat test. The tops of the conical flasks were wrapped with aluminium foil, and they were placed in an orbital shaker (Thermoline TS-400) set at 180 rpm. The samples were shaken for 48 hours. After the completion of trials, solid adsorbents were separated using 0.45-micron polyethersulfone (PES) membrane filter paper. The filtrates as well as raw samples were then sent to ALS Limited, Australia for analysis. The adsorption of PFASs by various adsorbent materials was determined using the ALS generated data.

## 3. Results and discussion

### 3.1. Process stability

Process stability with respect to important process parameters such as temperature and O<sub>2</sub> concentration is vital in obtaining products of desired quality as well as maintaining the energy balance of the semi-pilot pyrolysis unit. The integration and operation of pyrolysis–combustion has been demonstrated in fixed bed and Auger type reactor designs in the literature.<sup>53</sup> However, an integrated fluidised bed pyrolysis–combustion process has not been demonstrated yet in the literature. The present work demonstrated a stable

**Table 2** Concentrations of various PFASs in contaminated water

Species	Chemical formula	Concentration (µg L <sup>-1</sup> )	
		Sample 1	Sample 2
Perfluorooctanesulfonic acid (PFOS)	F(CF <sub>2</sub> ) <sub>8</sub> SO <sub>3</sub> H	480	0.08
Perfluorooctanoic acid (PFOA)	F(CF <sub>2</sub> ) <sub>7</sub> COOH	24	0.36
Perfluorohexanesulfonic acid (PFHxS)	F(CF <sub>2</sub> ) <sub>6</sub> SO <sub>3</sub> H	210	0.61
Perfluorobutanesulfonic acid (PFBS)	F(CF <sub>2</sub> ) <sub>4</sub> SO <sub>3</sub> H	80	0.05
Perfluoropentanesulfonic acid (PFPeS)	F(CF <sub>2</sub> ) <sub>5</sub> SO <sub>3</sub> H	56	—
Perfluoroheptanesulfonic acid (PFHpS)	F(CF <sub>2</sub> ) <sub>7</sub> SO <sub>3</sub> H	20	—
Perfluorododecanoic acid (PFDaA)	F(CF <sub>2</sub> ) <sub>11</sub> COOH	0.22	—
Perfluorotridecanoic acid (PFTrDA)	F(CF <sub>2</sub> ) <sub>12</sub> COOH	0.07	—
Perfluorotetradecanoic acid (PFTeDA)	F(CF <sub>2</sub> ) <sub>13</sub> COOH	0.07	—

integrated fluidised bed pyrolysis–combustion system that can achieve highly stable temperature and oxygen concentration profiles. The advantage of such an integrated process is the compact design which can help reduce the capital and operating costs as well as improve the product quality.

Fig. 2 shows an illustrative presentation of the temperature profiles of various thermocouples as well as the O<sub>2</sub> concentration profile during a trial performed at 600 °C. Temperature fluctuation was found to be minimal. In addition, the O<sub>2</sub> concentration was far below 1% during the entire trial and, consequently, the process atmosphere was nearly inert. This demonstrates that this technology offers a stable process for biochar production.

The monitoring of major components of flue gas during the trial is shown in Fig. 3. The concentration of CO<sub>2</sub> ranged between 13 and 15%. This range of CO<sub>2</sub> values provides a justification for choosing a mixture of 85% N<sub>2</sub> and 15% CO<sub>2</sub> as the fluidising gas. The concept applied here is that the flue gas may be recycled and utilised as the fluidising gas.

The gas analysis was performed at the stack. The level of SO<sub>2</sub> was observed to be very low (4–10 ppm) in all of our trials. NO<sub>x</sub> was also low and in the range of 120 to 125 ppm while CO was between 40 and 50 ppm (Fig. 3). The concentrations of hydrocarbons were also measured; however, the values were not detectable and therefore, not reported here. These values were found to be well below the emission limits recommended by the Industrial Emissions Directive (IED) 2010/75/EU.

### 3.2. Product distribution of py-oil

The analysis of the scrubber water sample (*i.e.*, product distribution of py-oil) is shown in Fig. 4. The Py-oil components were divided into six major groups, which include polyaromatic hydrocarbons (PAHs), monoaromatic hydrocarbons (MAHs), alcohols, phenols, and C10–C14 and C15–C28 liquid hydrocarbons. This grouping was done following previous studies.<sup>54,55</sup> It was found that the

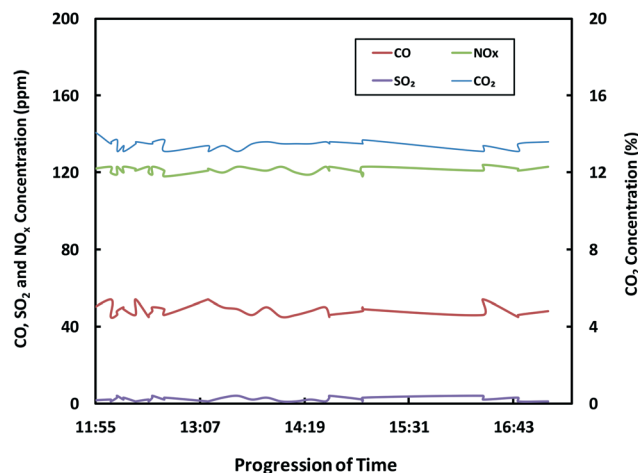


Fig. 3 Analysis of flue gas using an online IR analyser for the 600 °C trial.

production of PAHs and MAHs were minimal in the py-oil sample. The major components of py-oil were hydrocarbons followed by alcohols and phenols. This product distribution is favourable if py-oil is considered for combustion to provide energy to the pyrolysis system.

While the py-oil product distribution is favourable in the context of combustibility, it will still require pre-treatment before it can be used as a fuel in traditional power generators.<sup>24</sup> A better approach could be combusting py-oil to provide energy to the pyrolysis process. In the current semi-pilot plant, a lower combustion temperature was applied with the intention to investigate PFAS destruction. In the real world, a higher combustion temperature could be applied which would combust py-oil and py-gas and provide the required energy to the system.

### 3.3. Yield and stability of biochar

The biochar yield against pyrolysis temperature is shown in Fig. 5. In this study, py-gas and py-oil were partially

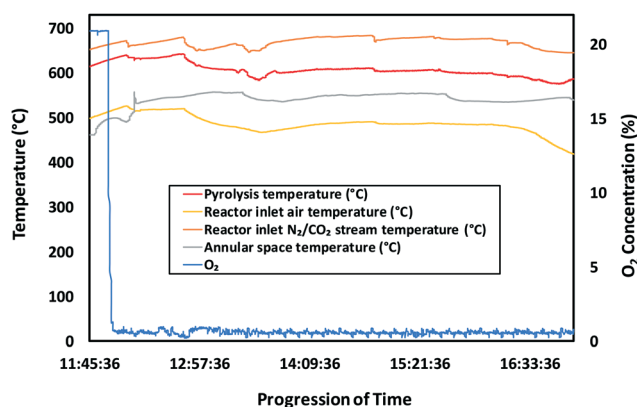


Fig. 2 Temperature profiles and oxygen concentration (in the pyrolysis zone) for the 600 °C trial.

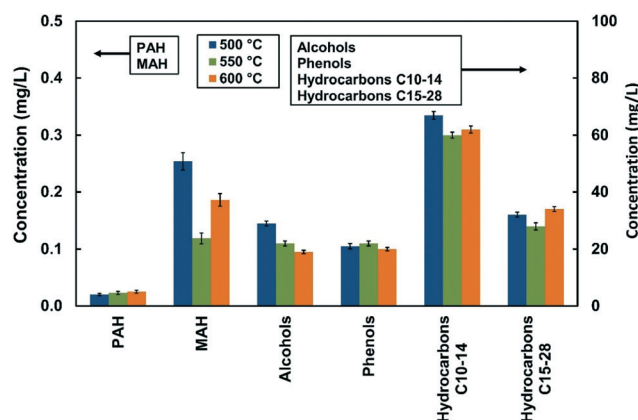


Fig. 4 Analysis of the scrubber water sample (product distribution of py-oil).

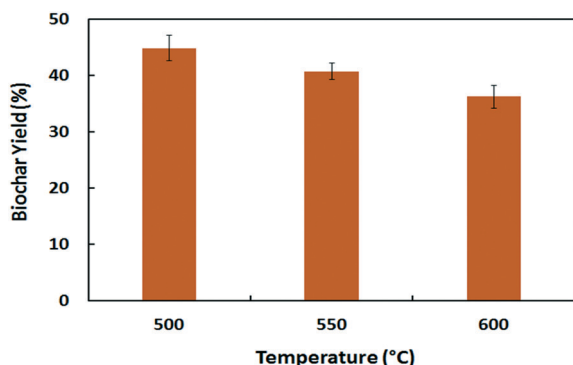


Fig. 5 Biochar yield against pyrolysis temperature.

combusted. The uncombusted py-oil was captured in the water scrubber while uncombusted py-gas was detected in the flue gas. As the combusted portion was not measured, the determination of yields of py-gas and py-oil was not possible. Therefore, biochar yield data are only obtained and presented. Pyrolysis of biosolids results in the decomposition of carbohydrates, proteins, lipids, polyphenols and other macromolecular humic substances as well as microorganisms.<sup>56,57</sup> The level of decomposition of these species increases with pyrolysis temperature, leading to lower biochar yield.

The effects of pyrolysis temperature on biochar formation is further reflected by the proximate and ultimate analyses of the biochar samples (Table 3). As expected, with the increase of temperature, the volatile matter and fixed carbon decreased while the ash content increased. According to the ultimate analysis, C, H and N decreased with the increase of temperature. However, the variation of S was found to be minimal in the investigated temperature regime. This suggests that the sulphur containing species do not degrade significantly within the temperature regime investigated. The proximate and ultimate analyses of biosolids and biochar were also used to construct a Van Krevelen diagram (Fig. S3†). This diagram is an illustration of the maturity/stability of biochar materials.<sup>58</sup> Both H/C and O/C ratios decreased significantly from biosolids to biochar as confirmed in Fig. S3.†

The detailed transition of H/C and O/C values from biosolids to biochar is shown in Table 4. It was found that both ratios decreased with the increase of pyrolysis temperature. A similar result was reported by Fryda and Visser.<sup>58</sup> This was possible because demethylation (loss of

Table 4 H/C and O/C mole ratios of biosolids and biochar

	Biosolids	BSBC-500	BSBC-550	BSBC-600
H/C mole ratio	1.4726	0.6800	0.6761	0.6087
O/C mole ratio	0.4116	0.0125	0.0111	0.0095

BSBC-500: biochar produced at 500 °C, BSBC-550: biochar produced at 550 °C, BSBC-600: biochar produced at 600 °C.

CH<sub>3</sub>) and decarboxylation (loss of CO<sub>2</sub>) reactions are enhanced with the increase of pyrolysis temperature. The increase of demethylation reactions decreases the H/C ratio while the increase in decarboxylation reactions reduces the O/C ratio.<sup>59</sup>

The highest H/C mole ratio was found to be 0.68 for the biochar produced at 500 °C and this value was lower than that from the International Biochar Initiative guidelines (the suggested maximum H/C mole ratio by the guidelines is 0.7).<sup>60</sup> The highest O/C mole ratio was 0.0125 for the biochar produced at 500 °C. This O/C ratio value is in the lower range when compared to that of other biochar samples, and this seems indicative of a very long half-life (more than 1000 years) when added to soil.<sup>61</sup> Therefore, it is worth noting that the produced biochar samples are very stable carbon materials and suitable for soil carbon sequestration.

### 3.4. Biochar morphology and surface area

The morphological analyses of biochar produced at 500, 550 and 600 °C were performed using a scanning electron microscope (SEM) (Fig. 5). It can be seen that a porous structure was evident at all temperatures and the porosity was found to increase slightly with the increase in temperature from 500 to 600 °C. The BET surface area of the biochar samples was measured and the values obtained are in the range of 26 to 55 m<sup>2</sup> g<sup>-1</sup> (mean values were 26.45, 44.06 and 55.29 m<sup>2</sup> g<sup>-1</sup> for the 500, 550 and 600 °C trials, respectively). These values are well aligned with the SEM findings.

The particle size distributions of biosolids and biochar particles are shown in Fig. 7. It was found that the particle size decreases from biosolids to biochar. The median value (for a volume distribution value), *D<sub>v</sub>* (50), decreased from 829 to 587 μm. *D<sub>v</sub>* (50) represents the median value for a volume distribution. As shown in Fig. 6, the biochar yield was in the range of 36–45%, depending on temperature. This huge

Table 3 Proximate and ultimate analyses of biochar

Sample	Proximate analysis <sup>a</sup> (%)				Ultimate analysis <sup>a</sup> (%)				
	Moisture	Volatiles	Ash	Fixed carbon	C	H	N	S	O <sup>b</sup>
BSBC-500	1.7	13.2	64.88	19.1	29.27	1.66	3.25	0.46	0.49
BSBC-550	1.3	12.1	66.77	21.4	28.01	1.58	2.78	0.44	0.41
BSBC-600	2.0	10.9	68.03	10.9	27.21	1.38	2.60	0.43	0.35

<sup>a</sup> Values on a dry weight basis. <sup>b</sup> Value determined by difference; BC-500 represents biochar produced at the pyrolysis temperature of 500 °C and similar definitions apply for BC-550 and BC-600.

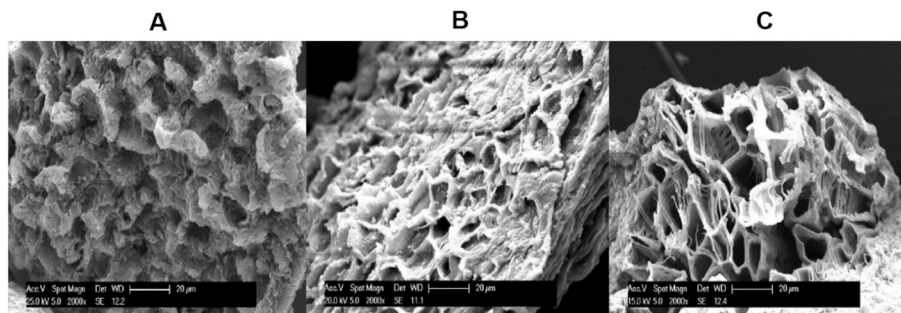


Fig. 6 SEM images of the biochar samples: (A) BSBC-500, (B) BSBC-550 and (C) BSBC-600.

percentage reduction of mass leads to a decrease in solid particle size as confirmed by the particle size distribution results. The bulk densities of solid particles were also reduced. The bulk density of 0.5–2 mm biosolids was found to be  $660 \text{ kg m}^{-3}$ , while the biochar obtained from the pyrolysis of these biosolids at  $500 \text{ }^\circ\text{C}$  exhibited a bulk density of  $620 \text{ kg m}^{-3}$ .

### 3.5. Heavy metal composition

The concentrations of various heavy metals in the biosolids employed and biochar samples produced from the trials are presented in Table 5. Also, the allowable concentrations of heavy metals for land application suggested by EPA Victoria (for biosolids)<sup>62</sup> and the International Biochar Initiative<sup>60</sup> are also provided for comparison. Contamination grade 1 (C1) biosolids, as per the EPA Victoria guidelines, correspond to the highest quality biosolids consisting of the lowest level of heavy metal contamination, and therefore, they are allowed to be used in land application without any specific control measures. In contrast, contamination grade 2 (C2) biosolids are allowed with controlled application.

The mass and volume reduction from biosolids to biochar during the pyrolysis process increased the concentrations of heavy metals. The only exception observed was Hg. This is because of the lower boiling point of Hg, leading to vapourisation of this element at the studied pyrolysis temperatures. While the heavy metal concentrations

increased in biosolids biochar, the values were still below the threshold values of the C2 grade suggested by the EPA Victoria and International Biochar Initiative guidelines.

### 3.6. Destruction of biosolids PFASs

Fig. 8 highlights the PFAS analysis data for biosolids, biochar and scrubber water. While the concentrations of a majority of PFAS species in the biosolids were found to have definite values, all PFAS species were extremely low (less than detectable values) in both biochar and scrubber water. This confirmed that PFASs were vapourised from biosolids at pyrolysis temperature leading to the production of nearly PFAS free biochar. Similar findings were published by Bioforcetech.<sup>63,64</sup> The extremely low concentrations of PFAS species in both biochar and scrubber water suggest that several PFAS species might have been partially or completely destroyed in the integrated pyrolysis–combustion environment maintained in the pyrolysis reactor and its adjacent annular space. Temperature, gas residence time, oxygen, water vapour and the gas phase chemistry of alkali and alkaline earth minerals (*i.e.* K, Na, Ca, and Mg) might have played critical roles in PFAS destruction followed by mineralisation. The roles of temperature and residence time are well-known as higher temperature and residence times can improve the destruction kinetics.<sup>65</sup> The literature has demonstrated that oxygen and water vapour can play critical roles in the destruction of fluorinated hydrocarbons.<sup>66,67</sup> In a similar way, oxygen and water vapour (generated from combustion of pyrolysis gas vapours) can play important roles in PFAS destruction. The release of alkali and alkaline earth minerals into the vapour phase and their gas phase chemistry with PFASs and destructed fluorine can also enhance PFAS destruction and mineralisation efficiency.<sup>66,68</sup> There is also a possibility that PFASs might have converted into some unknown organofluorine compounds which might not be in the analytical range.<sup>26,69</sup> Such compounds could be gaseous organofluorocarbons such as  $\text{CF}_4$  and  $\text{C}_2\text{F}_6$ . Unfortunately, the nature of the semi-pilot scale trials presented in this work did not allow the authors to investigate the role of each of these parameters in detail.

Mass balance for PFASs could not be developed for the semi-pilot trials as several PFAS concentration values in the

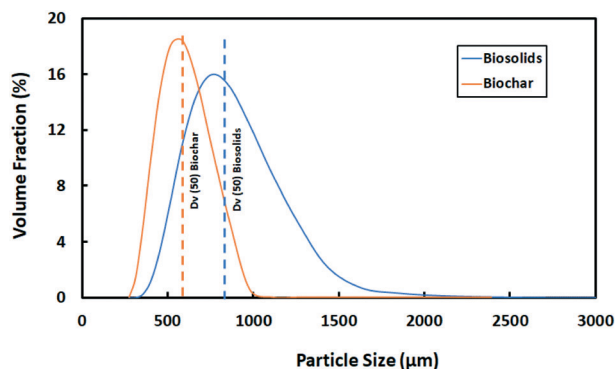


Fig. 7 Particle size distributions of biosolids and biochar.



**Table 5** Total metal concentrations ( $\text{mg kg}^{-1}$ ) of the biosolids and corresponding biochar samples

Metals	BS	BSBC-500	BSBC-550	BSBC-600	C1 grade <sup>a</sup>	C2 grade <sup>a</sup>	Biochar guidelines <sup>b</sup>
As	<5	5	5	<5	20	60	13–100
Cd	1.4	1.9	1.6	1.6	1	10	1.4–39
Cr	24	44	50	78	400	3000	93–1200
Cu	660	1100	1200	1100	100	2000	143–6000
Pb	19	40	42	39	300	500	121–300
Hg	0.79	<0.05	<0.05	<0.05	1	5	1–17
Ni	18	37	68	180	60	270	47–420
Se	6	6	6	5	3	50	2–200
Zn	870	1600	1700	1700	200	2500	416–7400

BS: biosolids. <sup>a</sup> EPA Victoria Biosolids guidelines. <sup>62</sup> <sup>b</sup> International Biochar Initiative guidelines. <sup>60</sup>

liquid and biochar samples were not specific. However, attempts were made to gain some understanding on PFAS removal efficiency (Table S2†). In this estimation, the concentration values, shown with the ‘<’ sign in Table S1† (also presented in Fig. 8 with a marker), were considered as the final concentration values for PFASs. For instance, the concentration of PFOS in biochar was  $<0.0002 \text{ mg kg}^{-1}$  (Table S1†). In the estimation, the concentration of PFOS was considered as  $0.0002 \text{ mg kg}^{-1}$ . This estimation provides the removal values of PFBS, PFOS, PFPeA, PFHxA, PFHpA and PFOA as follows: 74, 98, 75, 84, 54 and 96%, respectively. While this is a very rough estimation, this still tells that several PFASs were removed in the pyrolysis process. The removal of other PFAS compounds was either low or they were forming during the process.

To confirm this as well as to explore the mechanism of PFAS destruction, more scientific experiments would be required in the future. As described previously, closing the mass balance for all PFASs was extremely difficult due to the low values of PFASs in the initial biosolids samples. A practical method for the way forward could be performing systematic spiking experiments (*i.e.* spike different PFASs into biosolids) in a lab-environment in a more controlled

manner as spiking at a semi-pilot or pilot scale can be very challenging. Lab-scale spiking experiments in a controlled environment may help not only in closing the mass balance but also in exploring the reaction mechanism of PFAS destruction in biosolids pyrolysis, where the feed material is highly heterogeneous, including organic and inorganic materials.

From this study, the authors would like to highlight that PFASs in biosolids, when compared with pure PFASs, might not require higher temperatures (*i.e.*  $\sim 1000 \text{ }^\circ\text{C}$  for pure PFASs<sup>70</sup>) for their destruction due to the different gas-phase chemistry and potential catalytic effects of minerals/heavy metals present in the biosolids. More scientific work will be required to investigate this fundamentally. Specifically, spiking experiments with particular PFAS compounds at the lab scale in a controlled environment are desirable to evaluate the destruction and mineralisation efficiency and mechanism.

### 3.7. PFAS adsorption

The adsorption efficiency (% adsorption) of char materials for PFASs of contaminated water samples (*i.e.*, sample 1 and sample 2) is shown in Fig. 9. For this study, BSBC-600 and BMBC-600 were used. It is well known that pH has a great impact on the adsorption of PFASs.<sup>22,71</sup> This has also been reflected in the present study. For example, there was a higher PFOS adsorption efficiency for sample 1 compared to that for sample 2. This was due to the lower pH of sample 1 than that of sample 2 (4.3 vs. 7.85), and this is consistent with the literature.<sup>71</sup> At low pH of the contaminated water sample, electrostatic attraction between the positively charged adsorbent surface and the negatively charged PFOS molecules is strong,<sup>72</sup> and this assists in enhanced adsorption of PFOS molecules.

The length of PFAS chains has significant impacts on PFAS adsorption. Short-chain PFASs are difficult to adsorb by many adsorbents, including commercially available granular activated carbon (GAC). For example, perfluorobutanesulfonic acid (PFBS) is a C4 PFAS. The adsorption efficiency of these species by both BSBC and BMBC is low with a range of 19–27% (Fig. 9a). However, the adsorption efficiency of PFBS was

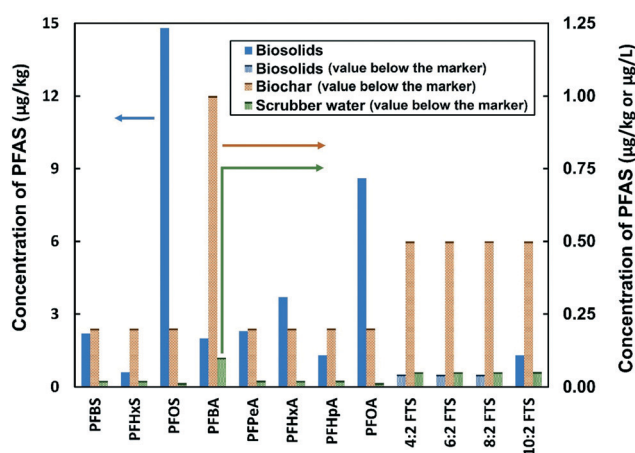


**Fig. 8** PFAS concentration data for biosolids ( $\mu\text{g kg}^{-1}$ ), biochar ( $\mu\text{g kg}^{-1}$ ) and scrubber water ( $\mu\text{g L}^{-1}$ ). Columns with markers represent values less than the marker values (see detailed data in Table S1†).

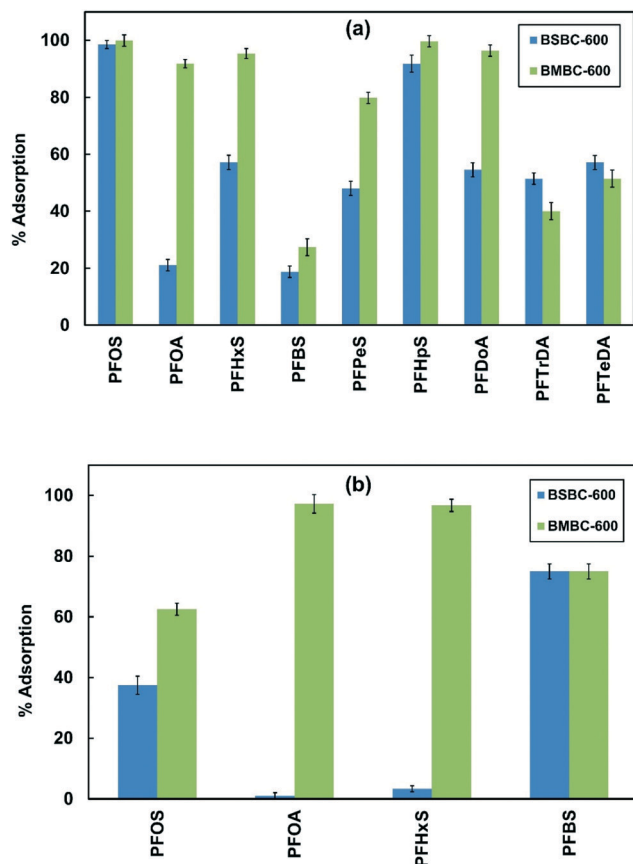


Fig. 9 PFAS adsorption efficiency by various char samples: (a) contaminated water sample with high concentration (*i.e.*, sample 1) and (b) contaminated water sample with low concentration (*i.e.*, sample 2). Note that BSBC represents biosolids biochar, and BMBC represents biomass biochar.

found to increase for the low concentration sample with both adsorbents (Fig. 9b). Using the BSBC adsorbent, the effect of concentration on the adsorptions of PFOS, PFOA and PFHxS was found to be the opposite of that for PFBS. With the decrease of concentration, the adsorption of the three PFASs decreased when BSBC was applied. The impact of concentration on PFAS adsorption with BMBC was found to be relatively low. This is most likely due to the higher surface area of BMBC (BET surface area, BMBC-600:  $79.87 \text{ m}^2 \text{ g}^{-1}$ ; BSBC-600:  $55.29 \text{ m}^2 \text{ g}^{-1}$ ). This finding is aligned with a previous study conducted by Bentley *et al.* who investigated micropollutant adsorption using biosolids biochar and pine biochar.<sup>73</sup>

The terminal functional groups may have an impact on PFAS adsorption. Regardless of concentration, BSBC underperformed in PFOA adsorption when compared to BMBC. It appears that PFASs with carboxylic acids as functional groups have lower adsorption affinity to BSBC. However, the difference of adsorption affinity between BSBC and BMBC becomes very low for PFASs with sulphonic acids as a terminal functional group.

The hydrophobic interactions between PFASs and the adsorbent can assist in PFAS removal from contaminated

water as a hydrophilic functional group with a hydrophobic tail is present in PFASs.<sup>74,75</sup> Briefly, the hydrophobic surface of adsorbents enhances PFAS adsorption.<sup>76,77</sup> The metal content was higher in BSBC compared to BMBC. Therefore, it may be possible that the metals in BSBC reduce surface hydrophobicity and decrease the adsorption of PFASs.<sup>78</sup> This may be the reason for the higher PFAS adsorption on BMBC compared to that on BSBC. While BSBC did not perform as effectively as BMBC for adsorption of some PFASs, its production is expected to be comparatively less expensive. Therefore, a higher amount of BSBC can be applied solely or in combination with BMBC and high performing PFAS adsorbents such as GAC and resins. Also, selective application of BSBC for the adsorption of some PFASs such as PFOS and PFBS can also be considered.

## 4. Conclusions

A semi-pilot pyrolysis unit was employed for the transformation of biosolids into biochar. The semi-pilot unit achieved highly stable thermal and oxygen profiles in the pyrolysis zone. It was observed that with the increase of pyrolysis temperature, the biochar yield and fixed carbon in biochar decreased. It could be noted that the development of pores increased with the pyrolysis temperature. The produced biochar samples were stable and are expected to present a long half-life if used as soil additives. The heavy metal concentration in biochar increased, but it was within the EPA Victoria C2 biosolids grading and the guidelines provided by the International Biochar Initiative. The trials also demonstrated that integrated low-temperature pyrolysis-combustion might be an effective method for removing PFASs from biosolids by converting them into biochar. More scientific experiments in a controlled lab-environment are needed to confirm this.

Biosolids biochar was found to be an excellent adsorbent for removing PFASs from contaminated water. The benchmarking with biomass biochar suggested that the biomass biochar performed better in adsorbing PFASs when compared to the biosolids biochar. Despite this, the lower production cost of biosolids biochar might still make it attractive to be used at a commercial scale.

## Conflicts of interest

There are no conflicts of interest to declare.

## Acknowledgements

The authors wish to acknowledge the financial support received from South East Water, Intelligent Water Networks (IWN) and RMIT University.

## References

- 1 S. Patel, S. Kundu, P. Halder, L. Rickards, J. Paz-Ferreiro, A. Surapaneni, S. Madapusi and K. Shah, *Renewable Energy*, 2019, **141**, 707–716.

- 2 I. Fonts, G. Gea, M. Azuara, J. Ábrego and J. Arauzo, *Renewable Sustainable Energy Rev.*, 2012, **16**, 2781–2805.
- 3 P. Manara and A. Zabaniotou, *Renewable Sustainable Energy Rev.*, 2012, **16**, 2566–2582.
- 4 P. Darvodelsky, Department of Sustainability, Environment, Water, Populations and Communities, Website: <https://www.environment.gov.au/system/files/resources/2e8c76c3-0688-47ef-a425-5c89dff9e04/files/biosolids-snapshot.docx>, Accessed: 21 Oct 2019, 2011.
- 5 L. W. Jacobs and D. S. McCreary, *Utilizing biosolids on agricultural land*, Michigan State University Extension, 2001.
- 6 What are biosolids?, Australian & New Zealand Biosolids Partnership, Website: <https://www.biosolids.com.au/info/what-are-biosolids/>, Accessed: 21 Oct 2019.
- 7 M. Gong, W. Zhu, Z. Xu, H. Zhang and H. Yang, *Renewable Energy*, 2014, **66**, 605–611.
- 8 PFAS NEMP 2.0, Environment Protection Authority Victoria, Website: <https://www.epa.vic.gov.au/for-community/environmental-information/pfas/pfas-nemp-2-0>, Accessed: 25 June 2020.
- 9 T. L. Coggan, D. Moodie, A. Kolobaric, D. Szabo, J. Shimeta, N. D. Crosbie, E. Lee, M. Fernandes and B. O. Clarke, *Heliyon*, 2019, **5**, e02316.
- 10 O. A. Oyetade, G. B. B. Varadwaj, V. O. Nyamori, S. B. Jonnalagadda and B. S. Martincigh, *Rev. Environ. Sci. Bio/Technol.*, 2018, **17**, 603–635.
- 11 Basic Information on PFAS, United States Environmental Protection Agency, Website: <https://www.epa.gov/pfas/basic-information-pfas>, Accessed: 21 October 2019.
- 12 N. B. Saleh, A. Khalid, Y. Tian, C. Ayres, I. V. Sabaraya, J. Pietari, D. Hanigan, I. Chowdhury and O. G. Apul, *Environ. Sci.: Water Res. Technol.*, 2019, **5**, 198–208.
- 13 J. M. Graber, C. Alexander, R. J. Laumbach, K. Black, P. O. Strickland, P. G. Georgopoulos, E. G. Marshall, D. G. Shendell, D. Alderson and Z. Mi, *J. Exposure Sci. Environ. Epidemiol.*, 2019, **29**, 172–182.
- 14 C. E. Rockwell, A. E. Turley, X. Cheng, P. E. Fields and C. D. Klaassen, *Food Chem. Toxicol.*, 2017, **100**, 24–33.
- 15 V. Berg, T. H. Nøst, S. Hansen, A. Elverland, A.-S. Veyhe, R. Jorde, J. Ø. Odland and T. M. Sandanger, *Environ. Int.*, 2015, **77**, 63–69.
- 16 M.-A. Verner, A. E. Loccisano, N.-H. Morken, M. Yoon, H. Wu, R. McDougall, M. Maisonet, M. Marcus, R. Kishi and C. Miyashita, *Environ. Health Perspect.*, 2015, **123**, 1317–1324.
- 17 E. C. Bonefeld-Jørgensen, M. Long, S. O. Fredslund, R. Bossi and J. Olsen, *Cancer Causes Control*, 2014, **25**, 1439–1448.
- 18 O. S. Arvaniti and A. S. Stasinakis, *Sci. Total Environ.*, 2015, **524**, 81–92.
- 19 A. K. Venkatesan and R. U. Halden, *J. Hazard. Mater.*, 2013, **252**, 413–418.
- 20 J. A. Sleep and A. L. Juhasz, *Environ. Pollut.*, 2020, 115120.
- 21 R. Mahinroosta and L. Senevirathna, *J. Environ. Manage.*, 2020, **255**, 109896.
- 22 I. Ross, J. McDonough, J. Miles, P. Storch, P. Thelakkat Kochunarayanan, E. Kalve, J. Hurst, S. S. Dasgupta and J. Burdick, *Remed. J.*, 2018, **28**, 101–126.
- 23 C. D. Vecitis, H. Park, J. Cheng, B. T. Mader and M. R. Hoffmann, *Front. Environ. Sci. Eng. China*, 2009, **3**, 129–151.
- 24 Z. Liu, P. McNamara and D. Zitomer, *Environ. Sci. Technol.*, 2017, **51**, 9808–9816.
- 25 F. Wang, X. Lu, X.-y. Li and K. Shih, *Environ. Sci. Technol.*, 2015, **49**, 5672–5680.
- 26 F. Wang, K. Shih, X. Lu and C. Liu, *Environ. Sci. Technol.*, 2013, **47**, 2621–2627.
- 27 Z. Liu, S. Singer, D. Zitomer and P. McNamara, *Catalysts*, 2018, **8**, 524.
- 28 S. Patel, S. Kundu, P. Halder, G. Veluswamy, B. Pramanik, J. Paz-Ferreiro, A. Surapaneni and K. Shah, *J. Anal. Appl. Pyrolysis*, 2019, 104697.
- 29 H. Wang, K. Lin, Z. Hou, B. Richardson and J. Gan, *J. Soils Sediments*, 2010, **10**, 283–289.
- 30 Y. Tong, B. K. Mayer and P. J. McNamara, *Environ. Sci.: Water Res. Technol.*, 2016, **2**, 761–768.
- 31 K. Bondarczuk, A. Markowicz and Z. Piotrowska-Seget, *Environ. Int.*, 2016, **87**, 49–55.
- 32 J. Ross, D. Zitomer, T. Miller, C. Weirich and P. J. McNamara, *Environ. Sci.: Water Res. Technol.*, 2016, **2**, 282–289.
- 33 T. Hoffman, D. Zitomer and P. J. McNamara, *J. Hazard. Mater.*, 2016, **317**, 579–584.
- 34 L. K. Kimbell, A. D. Kappell and P. J. McNamara, *Environ. Sci.: Water Res. Technol.*, 2018, **4**, 1807–1818.
- 35 Q. Lin, G. Chen and Y. Liu, *J. Anal. Appl. Pyrolysis*, 2012, **94**, 114–119.
- 36 M. Sánchez, O. Martínez, X. Gómez and A. Morán, *Waste Manage.*, 2007, **27**, 1328–1334.
- 37 A. Sarkar, S. D. Sarkar, M. Langanki and R. Chowdhury, *J. Energy*, 2015, **2015**, 618940.
- 38 N. Bolan, B. Sarkar, Y. Yan, Q. Li, H. Wijesekara, K. Kannan, D. C. Tsang, M. Schauerte, J. Bosch and H. Noll, *J. Hazard. Mater.*, 2020, **401**, 123892.
- 39 N. Watanabe, S. Takemine, K. Yamamoto, Y. Haga and M. Takata, *J. Mater. Cycles Waste Manage.*, 2016, **18**, 625–630.
- 40 T. D. Bucheli, I. Hilber and H.-P. Schmidt, *Biochar for Environmental Management: Science, Technology and Implementation*, 2015, pp. 595–624.
- 41 C. Wang, Y. Wang and H. Herath, *Org. Geochem.*, 2017, **114**, 1–11.
- 42 B. R. Simoneit, in *PAHs and Related Compounds*, Springer, 1998, pp. 175–221.
- 43 M. Keiluweit, M. Kleber, M. A. Sparrow, B. R. Simoneit and F. G. Prahl, *Environ. Sci. Technol.*, 2012, **46**, 9333–9341.
- 44 P. Devi and A. K. Saroha, *Bioresour. Technol.*, 2015, **192**, 312–320.
- 45 H. Sun and Z. Zhou, *Chemosphere*, 2008, **71**, 2113–2120.
- 46 M. D. Holliday, *Masters thesis*, Air Force Institute of Technology (AFIT), USA, 2020.
- 47 C. J. Liu, D. Werner and C. Bellona, *Environ. Sci.: Water Res. Technol.*, 2019, **5**, 1844–1853.
- 48 C. Zeng, A. Atkinson, N. Sharma, H. Ashani, A. Hjelmstad, K. Venkatesh and P. Westerhoff, *AWWA Water Sci.*, 2020, **2**, e1172.

- 49 P. McCleaf, S. Englund, A. Östlund, K. Lindegren, K. Wiberg and L. Ahrens, *Water Res.*, 2017, **120**, 77–87.
- 50 C. J. Liu, D. Werner and C. Bellona, *Environ. Sci.: Water Res. Technol.*, 2019, **5**, 1844–1853.
- 51 X. Xiao, B. A. Ulrich, B. Chen and C. P. Higgins, *Environ. Sci. Technol.*, 2017, **51**, 6342–6351.
- 52 D. Zhang, Q. He, M. Wang, W. Zhang and Y. Liang, *Environ. Technol.*, 2019, 1–12.
- 53 Biosolids pyrolysis process, Bioforcetech, Website: <https://www.bioforcetech.com/pyrolysis.html>, Accessed: 9 Dec 2020.
- 54 I. Fonts, M. Azuara, L. Lázaro, G. Gea and M. Murillo, *Ind. Eng. Chem. Res.*, 2009, **48**, 5907–5915.
- 55 C. Jindarom, V. Meeyoo, T. Rirksomboon and P. Rangsunvigit, *Chemosphere*, 2007, **67**, 1477–1484.
- 56 I. Fonts, M. Azuara, G. Gea and M. Murillo, *J. Anal. Appl. Pyrolysis*, 2009, **85**, 184–191.
- 57 J. Jimenez, F. Vedrenne, C. Denis, A. Mottet, S. Délérís, J.-P. Steyer and J. A. C. Rivero, *Water Res.*, 2013, **47**, 1751–1762.
- 58 L. Fryda and R. Visser, *Agriculture*, 2015, **5**, 1076–1115.
- 59 K. Wiedner, C. Rumpel, C. Steiner, A. Pozzi, R. Maas and B. Glaser, *Biomass Bioenergy*, 2013, **59**, 264–278.
- 60 International Biochar Initiative. Standardized Product Definition and Product Testing Guidelines for Biochar That Is Used in Soil; IBI biochar standards, International Biochar Initiative, Victor, NY, USA, 2012.
- 61 K. A. Spokas, *Carbon Manage.*, 2010, **1**, 289–303.
- 62 Guidelines for Environmental Management: Biosolids Land Application; Publication 943, EPA Victoria, Victoria, Australia, 2004.
- 63 Pyrolysis, Bioforcetech Corporation, Website: <https://www.bioforcetech.com/pyrolysis.html>, Accessed: 04 August 2020.
- 64 Bioforcetech, C/CAG of San Mateo County, Website: [https://ccag.ca.gov/wp-content/uploads/2020/02/BFT\\_FEB\\_2020-1.pdf](https://ccag.ca.gov/wp-content/uploads/2020/02/BFT_FEB_2020-1.pdf), Accessed: 04 August 2020.
- 65 J. Cui, P. Gao and Y. Deng, *Environ. Sci. Technol.*, 2020, **54**, 3752–3766.
- 66 N. Watanabe, M. Takata, S. Takemine and K. Yamamoto, *Environ. Sci. Pollut. Res.*, 2018, **25**, 7200–7205.
- 67 A. Murphy, A. Farmer, E. Horrigan and T. McAllister, *Plasma Chem. Plasma Process.*, 2002, **22**, 371–385.
- 68 M. Y. Khan, S. So and G. da Silva, *Chemosphere*, 2020, **238**, 124615.
- 69 F. Wang, X. Lu, K. Shih and C. Liu, *J. Hazard. Mater.*, 2011, **192**, 1067–1071.
- 70 G. Goldenman, M. Fernandes, M. Holland, T. Tugran, A. Nordin, C. Schoumacher and A. McNeill, *The cost of inaction: A socioeconomic analysis of environmental and health impacts linked to exposure to PFAS*, Nordic Council of Ministers, 2019.
- 71 Y. Bei, S. Deng, Z. Du, B. Wang, J. Huang and G. Yu, *Water Sci. Technol.*, 2014, **69**, 1489–1495.
- 72 C. Y. Tang, Q. S. Fu, D. Gao, C. S. Criddle and J. O. Leckie, *Water Res.*, 2010, **44**, 2654–2662.
- 73 M. J. Bentley and R. S. Summers, *Environ. Sci.: Water Res. Technol.*, 2020, **6**, 635–644.
- 74 Z. Du, S. Deng, Y. Bei, Q. Huang, B. Wang, J. Huang and G. Yu, *J. Hazard. Mater.*, 2014, **274**, 443–454.
- 75 D. Zhang, W. Zhang and Y. Liang, *Sci. Total Environ.*, 2019, 133606.
- 76 X. Chen, X. Xia, X. Wang, J. Qiao and H. Chen, *Chemosphere*, 2011, **83**, 1313–1319.
- 77 Q. Yu, R. Zhang, S. Deng, J. Huang and G. Yu, *Water Res.*, 2009, **43**, 1150–1158.
- 78 J. Chen, D. Zhu and C. Sun, *Environ. Sci. Technol.*, 2007, **41**, 2536–2541.